

Performance polyamides built on a sustainable carbohydrate core

Received: 14 July 2023

Accepted: 31 January 2024

Published online: 13 March 2024

Check for updates

Lorenz P. Manker¹, Maxime A. Hedou^{1,2}, Clement Broggi^{3,4}, Marie J. Jones^{1,5}, Kristoffer Kortsen⁶, Kalaiyarasi Puvanenthiran¹, Yildiz Kupper¹, Holger Frauenrath⁴, François Marechal⁵, Veronique Michaud³, Roger Marti², Michael P. Shaver⁶ & Jeremy S. Luterbacher¹✉

Sustainably producing plastics with performance properties across a variety of materials chemistries is a major challenge—especially considering that most performance materials use aromatic precursors that are still difficult to source sustainably. Here we demonstrate catalyst-free, melt polymerization of dimethyl glyoxylate xylose, a stabilized carbohydrate that can be synthesized from agricultural waste with 97% atom efficiency, into amorphous polyamides with performances comparable to fossil-based semi-aromatic alternatives. Despite the presence of a carbohydrate core, these materials retain their thermomechanical properties through multiple rounds of high-shear mechanical recycling and could be chemically recycled. Techno-economic and life-cycle analyses suggest selling prices close to those of nylon 66 with a reduction of global warming potential of up to 75%. This work illustrates the versatility of a carbohydrate moiety to impart performance that can compete with that of semi-aromatic polymers across two important materials chemistries.

Finding plastic precursors that can be synthesized with high efficiency from abundant, renewable feedstocks that are compatible with multiple material chemistries and that can offer performance properties akin to aromatic, phthalate-based monomers would greatly facilitate competition with petro-based products. Bio-based monomers on the Department of Energy's list of top value-added chemicals¹, notably 2,5-furandicarboxylic acid (FDCA), have been successfully used to create high-performance polyesters such as poly(ethylene furanoate). However, this molecule illustrates the challenge of finding versatile polymer precursors as its polymerization into useful polyamides has been hindered by incompatibility with the harsh reaction conditions of polyamide synthesis. For example, when polymerized with

diamines in the melt as is done industrially, FDCA tends to undergo substantial decarboxylation, resulting in low-molecular-weight polymers ($M_n < 10$ kDa) (refs. 2–6). Researchers have therefore resorted to solvent polymerization using Yamazaki–Higashi conditions^{7,8}, interfacial polymerization⁹ or enzymatic polymerization^{10,11} to study FDCA-based polyamides. However, these techniques are unlikely to be industrially viable, or sustainable, due to high solvent usage, the use of difficult-to-recycle catalysts/enzymes and increased downstream purification. Moreover, succinic acid, a less-rigid diacid on the Department of Energy's list of value-added chemicals from biomass, which also has a proven track record in synthesizing useful polyesters (for example, poly(butylene succinate)), similarly cannot currently

¹Laboratory of Sustainable and Catalytic Processing (LPDC), Institute of Chemicals Sciences and Engineering (ISIC), School of Basic Sciences (SB), Ecole Polytechnique Fédérale de Lausanne (EPFL), Lausanne, Switzerland. ²Institute of Chemical Technology, Haute Ecole d'Ingénierie et d'Architecture Fribourg, HES-SO University of Applied Sciences and Arts Western Switzerland, Fribourg, Switzerland. ³Laboratory for Processing of Advanced Composites (LPAC), Institute of Materials (IMX), School of Engineering (STI), Ecole Polytechnique Fédérale de Lausanne (EPFL), Lausanne, Switzerland. ⁴Laboratory of Macromolecular and Organic Materials (LMOM), Institute of Materials (IMX), École Polytechnique Fédérale de Lausanne (EPFL), Lausanne, Switzerland. ⁵Industrial Process and Energy Systems Engineering (IPESE), Ecole Polytechnique Fédérale de Lausanne (EPFL) Valais-Wallis, Sion, Switzerland. ⁶Department of Materials, Henry Royce Institute, The University of Manchester, Manchester, UK. ✉e-mail: jeremy.luterbacher@epfl.ch

be polymerized into high-molecular-weight polyamides due to intra-cyclization reactions at high temperatures. Even when direct solid-state polymerization is used to minimize these reactions, M_n s of only 8 kDa are achieved¹². Finding sustainable diacids that are compatible with both polyester and polyamide chemistries, akin to phthalic acids, is a notable challenge.

Producing sustainable monomers that can be incorporated into engineering polyamides could reduce the environmental footprint of this sector but also offers a higher-value market (as compared with commodity polyesters and polyolefins) to aid in the profitability of lignocellulosic biomass valorization, which is an ongoing challenge. Polyamide production currently faces substantial sustainability challenges, particularly in terms of global warming potential (GWP). For example, the most common polyamide, nylon 66 (PA-6,6), carries a GWP of 8–9 kgCO₂-equivalent (CO₂e) kg⁻¹ (for reference, polyethylene terephthalate has a GWP of 3 kgCO₂e kg⁻¹), with adipic acid carrying a large majority of the burden (GWP = 8.5 kgCO₂e kg⁻¹ adipic acid)¹³. Furthermore, polyamides are sold at high market prices, ranging from US\$3–7 kg⁻¹ for nylon 66 (refs. 14,15) to as high as US\$7–20 kg⁻¹ for the high-performance, semi-aromatic polyphthalamides (PPAs) based on phthalic acids, and their copolymers¹⁶. These factors could enable cost competitiveness of bio-based monomers, especially for high-performance specialty polyamides, while also offering large sustainability enhancements. In part for these reasons, there are already several commercial bio-based polyamides on the market, the large majority of which stem from the C₁₀ and C₁₁ acid/amine precursors that can be produced from castor oil (for example, PA-11; PA-10,10; PA-10,T; and so on). Despite their comparatively low mechanical strength and glass transitions relative to nylon 66, these materials offer performance advantages¹⁷ due to their exceptionally low water absorption and high flexibility, making them suitable for a range of applications, such as in specialty tubing (for example, fuel lines) or luxury sporting goods (for example, ski boots). However, there is still a lack of economically viable rigid, bio-based monomers for the synthesis of more high-performance polyamides with mechanical strengths and glass transitions akin to PPAs and their copolymers.

Building on a previously reported polymer precursor, dimethyl glyoxylate xylose (DMGX), that could be directly produced from abundant biomass at high yields and leads to degradable polyesters with well-rounded performance when polymerized with dialcohols¹⁸, in this Article, we demonstrate a simple synthetic pathway to also produce high-molecular-weight polyamides from DMGX in quantitative yields, in the melt at 250 °C, with three-hour reaction times and without a catalyst or specialized reactor systems. The incorporation of this largely unmodified natural carbohydrate cycle into the backbone of polyamides leads to performance properties competitive with those of complex amorphous engineering polyamides while enabling an efficient, atom-economical and sustainable synthesis from abundant renewable feedstocks. Mechanical testing demonstrates that these materials are sufficiently robust for industrial processing and several rounds of mechanical recycling. Alternatively, we introduce a process for chemical recycling these materials to monomers at yields >90% with straightforward downstream separations. Finally, we estimate selling prices to be in the range of commercial nylon 66 (US\$3–6 kg⁻¹, depending on the diamine used) with a 56–75% reduction in GWP (GWP), even when using fossil-derived glyoxylic acid (GA).

Results

Synthesis and characterization

In a previous study, we reported a scalable process to produce DMGX by acid-catalysed acetalization of xylose with GA, followed by esterification with methanol¹⁹. The DMGX product comprised a mixture of four stereoisomers and was purified by extraction, distillation and crystallization. The recrystallization parameters could also be adjusted to selectively crystallize the most prevalent stereoisomer

(SS isomer). This synthesis was demonstrated with a yield of 95% from purified xylose and a yield of 70–83% (molar basis from hemicellulose) when directly utilizing non-edible biomass such as wood or corn cobs. In addition to DMGX, this process generated a stabilized lignin²⁰ and a digestible cellulose as valuable co-products. This resulted in overall biomass utilization efficiencies (BUEs) of up to 86%, which represents the weight percentage of the cellulose, lignin and hemicellulose fractions that were successfully incorporated into valuable products. High BUEs are key to achieving both sustainability and profitability²¹ and are often low for bio-based aromatic plastic precursors. Bio-based terephthalic acid and FDCA have maximum theoretical BUEs of 42% and 59%, respectively, with actual efficiencies estimated to be on the order of 15–30% when produced industrially via 5-chloromethyl furfural²². Retaining the carbohydrate core within the polymer backbone via DMGX enables a theoretical BUE of 97% and an actual BUE of 80%, which has large implications in terms of cost and sustainability.

In this study, a series of polyamides were synthesized at 98–100% yield by direct melt polycondensation of crystalline DMGX with stoichiometric amounts of various aliphatic diamines (C₆, C₈, C₁₀ and C₁₂) in the presence of a secondary antioxidant (0.5 wt% triphenyl phosphite) and without addition of a polymerization catalyst (Fig. 1a). The antioxidant was used to prevent heavy discoloration of the polymer, probably by reducing hydroperoxide formation during polymerization. DMGX/diamine/triphenyl phosphite mixtures were heated to 140 °C under nitrogen and mechanical stirring, resulting in rapid reaction to form a white solid with distillation of methanol. Stirring was stopped, and the reaction temperature was then brought to 250–260 °C, where stirring was restarted to form a yellow/orange, viscous polymer melt. Discoloration during the melt polycondensation of polyamides by formation of conjugated species is a notorious problem and, in other systems, has been addressed by increased purification of the monomers combined with additive set optimization^{5,22}. Vacuum was then applied to drive the polycondensation, and the polymerizations were deemed complete when mechanical stirring became inefficient (total reaction time of 3–4 h). The polymers were directly discharged from the reaction flasks without dissolution/precipitation (see Supplementary Information 1.4.2 for detailed methods). The most-abundant single stereoisomer of DMGX (SS stereoisomer) was used for synthesis of the polyamides to simplify chemical characterization. The more industrially relevant four-stereoisomer DMGX mixture, which requires fewer separation steps and utilizes all four DMGX stereoisomers, was also used to synthesize one of the fully bio-based polyamides with bio-based 1,10-diaminodecane. We also scaled up the highest performing polyamide with 1,8-diaminooctane, both at a 400 g scale (Fig. 1e).

The molecular weights of the resulting polymers were determined via size-exclusion chromatography with multi-angle static light scattering (SEC-MALS) (Fig. 1b). All polymers from the single stereoisomer of DMGX (prefixed with IS hereafter) yielded high-molecular-weight polyamides (M_n = 20–30 kDa) with dispersities typical of a well-behaved polycondensation process (\mathcal{D} = 1.5–1.8). If higher molecular weights were desired, longer reaction times in high-torque industrial reactor systems could be used. However, this is unlikely to substantially enhance useful properties and would potentially decrease processability due to increased melt viscosities. The polymer produced from the four-stereoisomer mixture of DMGX and 1,8-diaminooctane at a 400 g scale, 4S-poly(octamethylene xylosediglyoxylamide) (4S PA-8,DGX), had an essentially identical molecular weight distribution as the single-isomer counterpart (IS PA-8,DGX) produced at a 35 g scale. The 4S-poly(decamethylene xylosediglyoxylamide) (4S PA-10,DGX) polymer also had a similar molecular weight to the corresponding single-isomer polymer (IS PA-10,DGX) but a higher dispersity (\mathcal{D} = 2.9). Full chemical characterization of the polyamides by nuclear magnetic resonance (NMR) spectroscopy (Fig. 1c and Supplementary Figs. 1–10) and matrix-assisted laser desorption-ionization time-of-flight mass spectrometry (MALDI-TOF-MS; Fig. 1d and Supplementary Fig. 11)

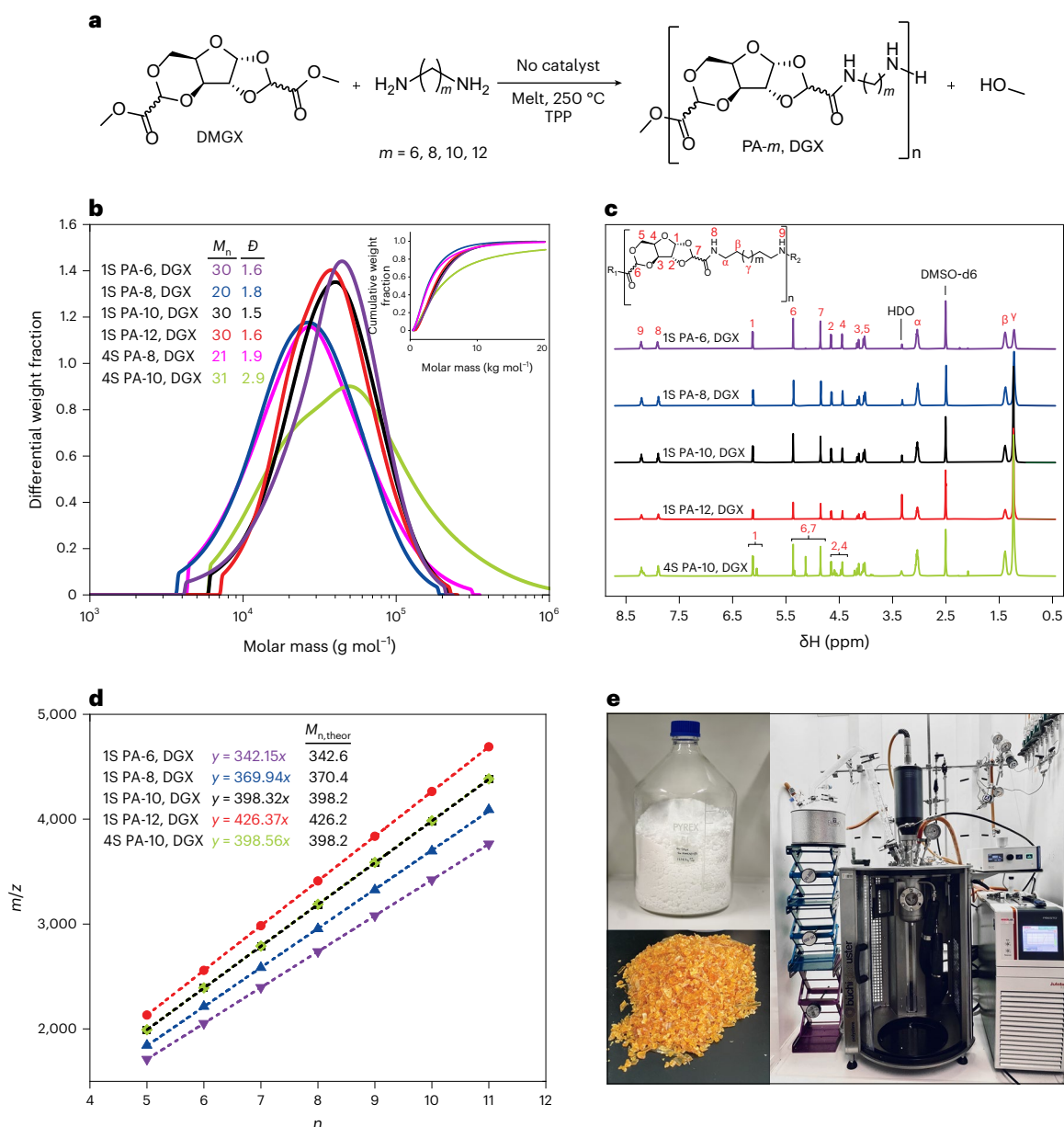


Fig. 1 | Synthesis and chemical characterization of the polyamides.

a, Polyamide synthesis. **b**, Molecular weight distributions. The inset shows the corresponding cumulative molecular weight distributions. **c**, $^1\text{H-NMR}$ spectra of all polyamides used in this study. **d**, Linear trendlines of MALDI-TOF-MS data with end group and ion weights subtracted. Mass-to-charge ratio (m/z) of detected

ions versus number of repeat units (n). All trendlines had regression coefficients of $R^2 = 1$. **e**, The crystalline 4S-DMGX (top left; 1.5 kg), the reactor used to produce the polyamides (right) and the final 4S PA-10, DGX polymer after grinding (bottom left). TPP, triphenyl phosphite.

revealed that the intended polymers were synthesized and with a final 1/1 stoichiometry of DMGX to diamine.

Material properties

The thermal properties of the polyamides were analysed using differential scanning calorimetry (DSC) and dynamic mechanical analysis (DMA; Supplementary Fig. 12), revealing amorphous polymers with glass transition temperatures ranging from 114 to 151 °C. These values are similar to those observed in semi-aromatic polyamides and substantially higher (by 44–110 °C) than the glass transition temperatures of commercial aliphatic polyamides (Fig. 2a). As water absorption (Supplementary Fig. 13) substantially impacts the glass transitions of polyamides, a detailed study into the thermo-mechanical properties of these polyamides in their dry, conditioned (equilibrated at 23 °C and 50% relative humidity (RH)) and

fully saturated (equilibrated in liquid water at 23 °C) states was also conducted via humidity-controlled DMA (see Supplementary Information 2.3 for extended text). Glass transition temperatures (by maximum of tangent delta curve) were 88–93 °C at 50% RH and 40–60 °C in the fully wet state (Supplementary Table 8). In the saturated wet state, however, the glass transition of 1S PA-6, DGX polymer dropped below room temperature so that the amorphous polymer became liquid, making it not useful for applications in the presence of water. Thermal gravimetric analysis (TGA) conducted under a nitrogen atmosphere indicated degradation onset temperatures (at 5% mass loss) and maximum degradation temperatures (at the maximum of the first derivative of the TGA curves) typical for polyamides, ranging from 364 to 385 °C and 410 to 423 °C, respectively (Supplementary Fig. 14). This demonstrates the impressive thermal stability of these materials, despite containing a nearly intact carbohydrate core. Gas barriers to oxygen and water,

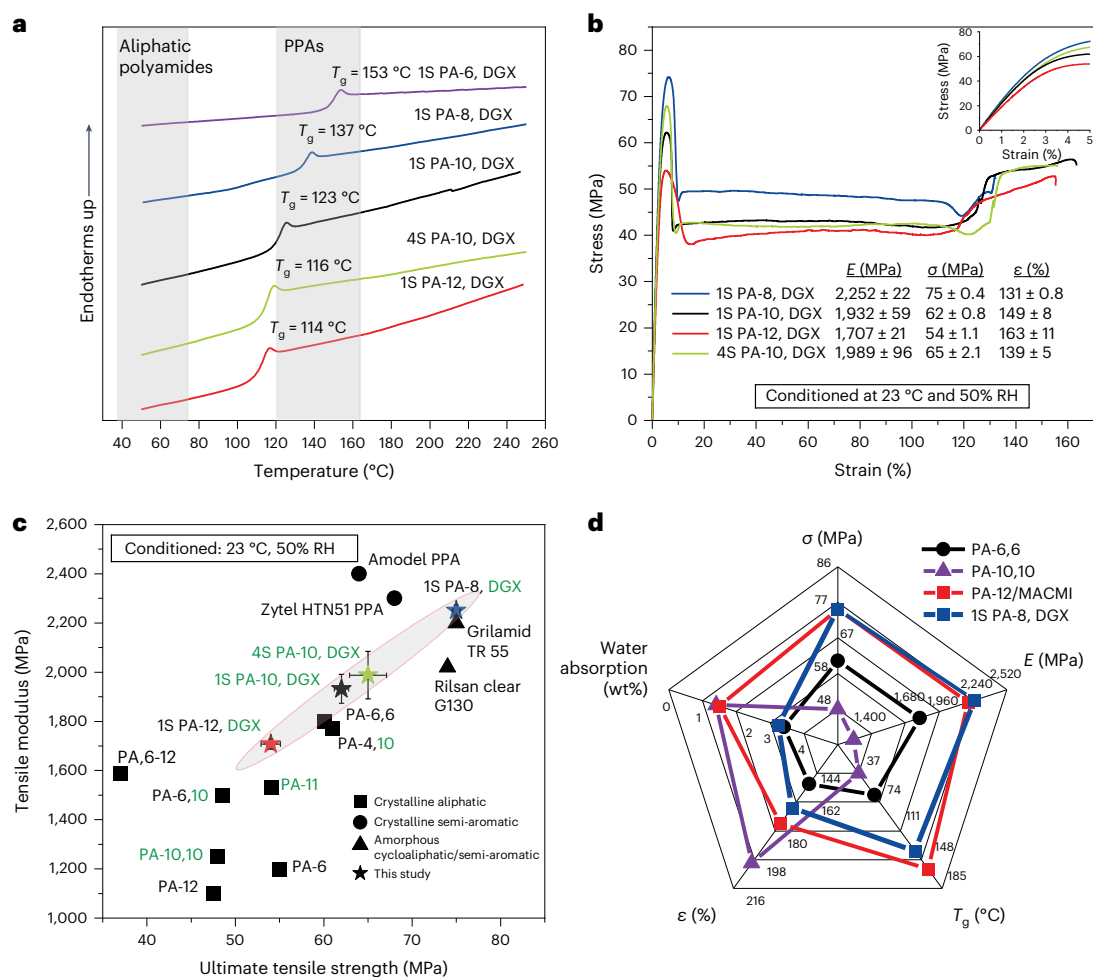


Fig. 2 | Thermomechanical properties of the polyamides. **a**, DSC chromatograms of dry polymers. **b**, Stress–strain curves of conditioned compression-moulded dogbones. The tabulated tensile values are averages with standard errors ($n = 3, 3, 4$ and 5 for the 1S PA-8, DGX, 1S PA-10, DGX, 1S PA-12, DGX and 4S PA-10, DGX polymers, respectively), and tensile curves are from single representative samples. **c**, Ashby plot benchmarking conditioned tensile properties against those of commercial polyamides. Green text indicates the polyamides or

monomers in the polyamides that are bio-based. References for commercial polyamide values can be found in Supplementary Table 9. Error bars are the standard errors reported in panel **b**. **d**, Radar chart comparing properties of 1S PA-8, DGX with nylon 66 (PA-6,6), a bio-based polyamide (PA-10,10) and a high-performance amorphous copolyamide (PA-12/MACMI). Mechanical properties are reported for the conditioned state (equilibrated at 23 °C and 50% RH). Glass transitions are for materials in the dry state.

while better than those of many bio-based plastics, remained below the range usually needed for thin food packaging (Supplementary Fig. 15)²³.

Tensile testing was conducted on compression-moulded dogbone samples that were conditioned at 23 °C and 50% RH. Interestingly, when the stretched tensile specimens were heated near the glass transition temperature, near-complete strain recovery was achieved, indicating a relaxation behaviour leading to shape recovery (refer to Supplementary Information 2.4 and Supplementary Fig. 16). The tensile results revealed high stiffness, strength and ductility ($E = 1,700$ – $2,250$ MPa, $\sigma = 54$ – 75 MPa, and $\epsilon = 140$ – 165%), with a final strain hardening observed in all samples (Fig. 2b). Injection-moulded dogbones of 4S PA-10, DGX exhibited a substantially higher tensile modulus ($E = 2,180$ MPa) compared with the compression-moulded samples ($E = 1,990$ MPa), but with slightly lower ultimate tensile strength ($\sigma = 61$ MPa versus 65 MPa) and elongation at break ($\epsilon = 64\%$ versus 139%), probably due to increased chain alignment from injection. As is typical for polyamides, tensile testing of dry, injection-moulded dogbones (Supplementary Fig. 17) led to a 38% increase in ultimate tensile strength ($\sigma = 84$ MPa versus 61 MPa), a slight increase in tensile modulus ($E = 2,273$ MPa versus 2,180 MPa) and a decrease in elongation at break ($\epsilon = 18\%$ versus 64%) as compared with the conditioned, injection-moulded specimens. This decrease in elongation at break upon drying is very comparable

to that of nylon 66, which decreases from $\epsilon = -150\%$ in the conditioned state to $\epsilon = 10$ – 45% in the dry state²⁴. A comparison of conditioned, room-temperature mechanical properties with commercial polyamides revealed mechanical strengths that could be tailored to range from those observed for typical aliphatic polyamides to those of semi-aromatic polyamides, depending on the diamine used (Fig. 2c). Achieving mechanical properties typically seen in semi-aromatic polyamides indicates that the inclusion of a polycyclic carbohydrate-based core within the polyamide backbone leads to mechanical strengths and stiffnesses that were previously achievable only by addition of aromatic monomers.

Comparison with incumbent materials

In applications involving the presence of liquid water, the PA-6, DGX polymers are unlikely to have notable mechanical utility, making PA-8, DGX the most high-performing polymer within this family of polyamides. A radar chart was used to benchmark the thermal, mechanical and water absorption properties of 1S PA-8, DGX with those of nylon 66, bio-based PA-10,10 and a commercial high-performance, amorphous, semi-aromatic copolyamide (Grilamid TR 55) that is very similar to the materials we report here (Fig. 2d). Grilamid TR is a class of high-performance copolyamide that is quite

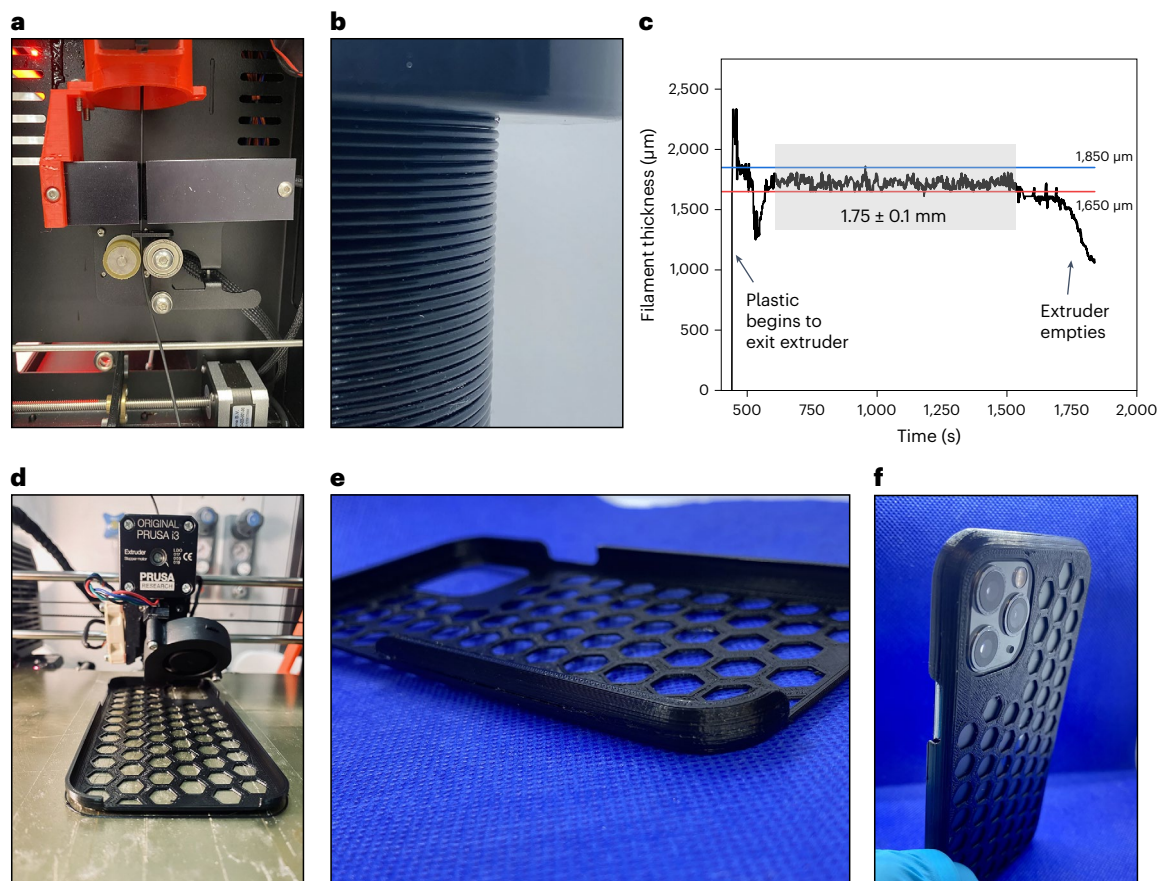


Fig. 3 | Filament production and fused-filament fabrication. **a**, Filament production via extrusion in a filament maker. **b**, The produced filament. **c**, Filament diameter measured over the course of the filament extrusion. **d**, Printing of an iPhone 11 pro case. **e, f**, The final 3D-printed phone case.

complex as it is composed of PA-12, a cycloaliphatic diamine called bis(methyl-para-aminocyclohexyl)methane (MACM) and isophthalic acid. The isomeric cycloaliphatic amine and the nonlinear isophthalic acid contribute to reduce crystallinity while simultaneously increasing the toughness and the glass transition of the material. This is very much in line with the effect of DMGX in the materials reported here. From the radar chart, it appears that DMGX-based polyamides could act as renewable alternatives to such high-performance, amorphous semi-aromatic polyamides. Alternatively, DMGX could be directly used in copolymer formulations as a replacement for, or complement to, isophthalic acid or cycloaliphatic diamines.

Processability

We produced a 400 g batch of 4S PA-10, DGX, which showed the relative ease of scale-up of this material, and we used this batch to demonstrate the processability of these polyamides. This polyamide was selected for demonstrating processability as it is the only polyamide that can be easily made fully bio-based and is the most representative material for this family of polyamides due to the intermediate length of the C_{10} diamine. A rheological master curve at a reference temperature of 250 °C showed that we had a viscous polymer with substantial shear thinning (complex viscosity drop from 10^5 Pa s at 0.1 rad s^{-1} to 10^3 Pa s at $1,000 \text{ rad s}^{-1}$) (Supplementary Fig. 18). The dried polyamide was processable by piston injection moulding at 260 °C and 1,000 bar (injection pressure) to produce tensile dogbone specimens and rheology discs (Supplementary Fig. 19) with only a 5% decrease in M_n (probably caused by thermomechanical shear and/or hydrolysis by absorbed water as is observed in other polyamide systems²⁵). The polyamide was also processed by high-shear twin-screw extrusion at 250 °C, 125 RPM with 7.8 Nm of torque and 30–50 bar die pressure to

produce filaments and pellets (Supplementary Figs. 20 and 21). As a proof of concept, the polyamide was then extruded with a polyethylene carbon-black masterbatch, pelletized to produce black pellets and then re-extruded at 250 °C in a filament maker to produce a 1.75 mm filament with good dimensional accuracy, within ± 0.1 mm diameter (Fig. 3a–c). Finally, additive manufacturing of an iPhone 11 pro case (Fig. 3d–f) by fused-filament fabrication was performed using a nozzle temperature of 275 °C and a bed temperature of 110 °C (the high temperature was used to prevent warping), demonstrating the ease of processability of the material.

Mechanical recycling

Considering that mechanical recycling is currently the most viable and sustainable method for recycling polymeric materials at their end-of-life stage²⁶, we investigated this recycling approach. Specifically, we subjected 4S PA-10, DGX to three cycles of high-shear twin-screw extrusion using an 11 mm diameter co-rotating twin-screw extruder with a length-to-diameter (L/D) ratio of 40, incorporating two mixing sections and one discharge section (Haake Process 11 parallel twin-screw extruder). To assess the retention of mechanical properties, injection-moulded tensile specimens were fabricated from the extrudate obtained from each cycle. Remarkably, the tensile properties remained nearly identical across the three cycles (Fig. 4a). Some degree of colouration was observed to increase slightly with each cycle (Supplementary Fig. 22); however, the initial orange colouration could potentially be avoided during synthesis through improved purification of diamines and additive formulation, in which case this discolouration could be avoided altogether. Post-extrusion, the polyamide was no longer fully soluble in a solvent and swelled to a greater degree with each extrusion cycle, suggesting some cross-linking reactions

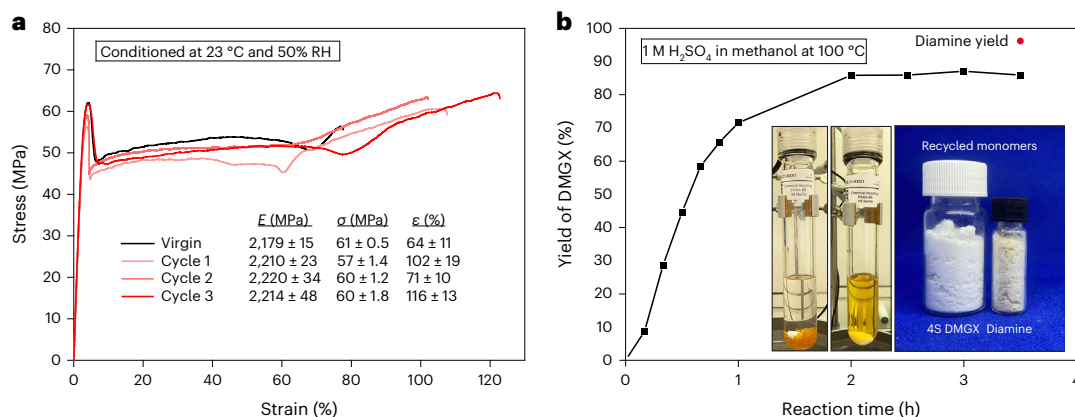


Fig. 4 | End-of-life options for PAX polyamides. **a**, Stress–strain curves of 4S PA-10,DGX over three cycles of high-shear extrusion at 250 °C. Tensile specimens were injection moulded. The tabulated tensile values are averages with standard errors ($n = 3, 3, 5$ and 3 for the virgin, cycle 1, cycle 2 and cycle 3 polymers, respectively), and tensile curves are from single representative samples. **b**, Kinetics of depolymerization of 4S PA-8,DGX by methanolysis. Data points are

from consecutive samples of individual reactions, and yields were determined by GC flame ionization detection with an internal standard. The diamine yield at the end of reaction (3.5 h) was determined by performing an identical reaction in deuterated solvents and using quantitative NMR with an internal standard. From left to right, the inset photos show the scaled chemical recycling reaction before reaction and after reaction and the resulting purified monomers.

occurred during extrusion, which again may be controlled by tuning additive sets as is done for polyolefin and polyester thermoplastics. Frequency-sweep rheology of the extrudates (Supplementary Fig. 23) revealed increases in zero-shear viscosity with each successive extrusion cycle but with relative increases diminishing between cycles—suggesting a plateau where chain scission and chain branching (including cross-linking) are balanced²⁷. However, at shear rates that are relevant to industrial processing ($10\text{--}10^4\text{ s}^{-1}$) (ref. 28), where shear thinning has a strong influence, the differences in viscosities between the different extrudates became far less notable. This indicates that only minor changes in processing conditions would be required in secondary manufacturing, as is the case for other common recyclates, such as polyethylene terephthalate²⁷. In our case, an increase of only 5 °C in the injection/mould temperatures was required for injection moulding of recycled dogbones as compared with the virgin material. Finally, we performed DSC and TGA on each of the recyclates and observed unsubstantial changes (for example, a 2 °C decrease in T_g) in the thermal properties as compared with the virgin material (Supplementary Fig. 24). Therefore, even if cross-linking reaction cannot be avoided by further optimization of extrusion conditions and/or additives, as the polymers remain reprocessable (injection moulding, extrusion and three-dimensional (3D) printing) and thermomechanical properties remain intact, cross-linking would probably limit only solvent casting or wet-spinning applications.

To ensure that cross-linking reactions did not occur during processing by compression/injection moulding and impact the properties measured in this study, SEC-MALS was performed on specimens before and after these processing steps. The results revealed slight decreases in M_n in post-processing specimens, with no visible fronting (that is, a high-molecular-weight shoulder) or back pressure during sample filtration (Supplementary Fig. 25). Together, these results indicate that these processing techniques did not likely introduce substantial branched or cross-linked populations that would impact thermomechanical properties.

Chemical recycling

We also explored chemical recycling as an end-of-life option (see Supplementary Fig. 26 for photos of the entire process). The poly(alkylene xylosediglyoxylate) (PAX) polyester counterparts were able to be chemically recycled using remarkably mild conditions (25 mM H_2SO_4 in methanol at 64 °C)¹⁹. Unsurprisingly, the amide linkages were substantially more stable than the esters and required high

concentrations of acid (1 M H_2SO_4) at 100 °C for depolymerization in reasonable time frames (<4 h; Fig. 4b). Nonetheless, high yields of DMGX (up to 90% by gas chromatography (GC)) and of 1,8-diaminooctane (96% by quantitative NMR; see Supplementary Information 1.4.5 for methods) were achieved. The slightly reduced yields of DMGX as compared with the diamine is probably due to ring opening of the acetal by residual water in these harsh conditions. This hypothesis is supported by the detection of ring-opened products by NMR analysis (Supplementary Fig. 27). On addition of dichloromethane (DCM) to the room-temperature reaction mixture, the sulfate salt of the diamine precipitated and was directly recovered with high purity (see Supplementary Fig. 28 for NMR). The filtrate was then concentrated and extracted with water to remove sulfuric acid and ring-opened products. Upon evaporation of the washed and dried DCM, crude DMGX was recovered in 78% isolated yield (91% separation yield; see Supplementary Fig. 29 for NMR). As a final polishing step, DMGX was recrystallized in ethanol in 88% yield (68% overall isolated yield; see Supplementary Fig. 29 for NMR). To recover the free diamine, the amine salt was basified with aqueous potassium hydroxide and extracted into DCM, yielding pure diamine in 61% overall isolated yield (see Supplementary Fig. 28 for NMR). The separation of monomers was not optimized but can probably be substantially improved, especially for the diamine, by optimizing precipitation conditions (for example, solvent, volume, temperature) and by performing at larger scale where transfer and hold-up losses become unsubstantial. In addition, as neutralization of the 1 M sulfuric acid was not necessary, there is potential for recycling of this stream. Although harsh, this recycling method would nevertheless be interesting for composites and multi-materials where mechanical recycling is less viable and where the recovery of internal components creates economic value.

TEA and LCA

A techno-economic analysis (TEA) for the production of 4S PA-8,DGX pellets was conducted to determine the economic feasibility of making this material (see Supplementary Information 2.1 for detailed TEA). A chemical plant producing 100,000 metric tons of 4S PA-8,DGX pellets per year was simulated in Aspen Plus (V12 Aspen Technology) using experimentally determined conditions and yields. The minimum selling price (MSP) of PA-8,DGX at the break-even point (internal rate of return = weighted average cost of capital) was calculated (Fig. 5a) for three different prices for 1,8-diaminooctane: US\$3.1 kg⁻¹ (corresponding to the average price of hexamethylenediamine in

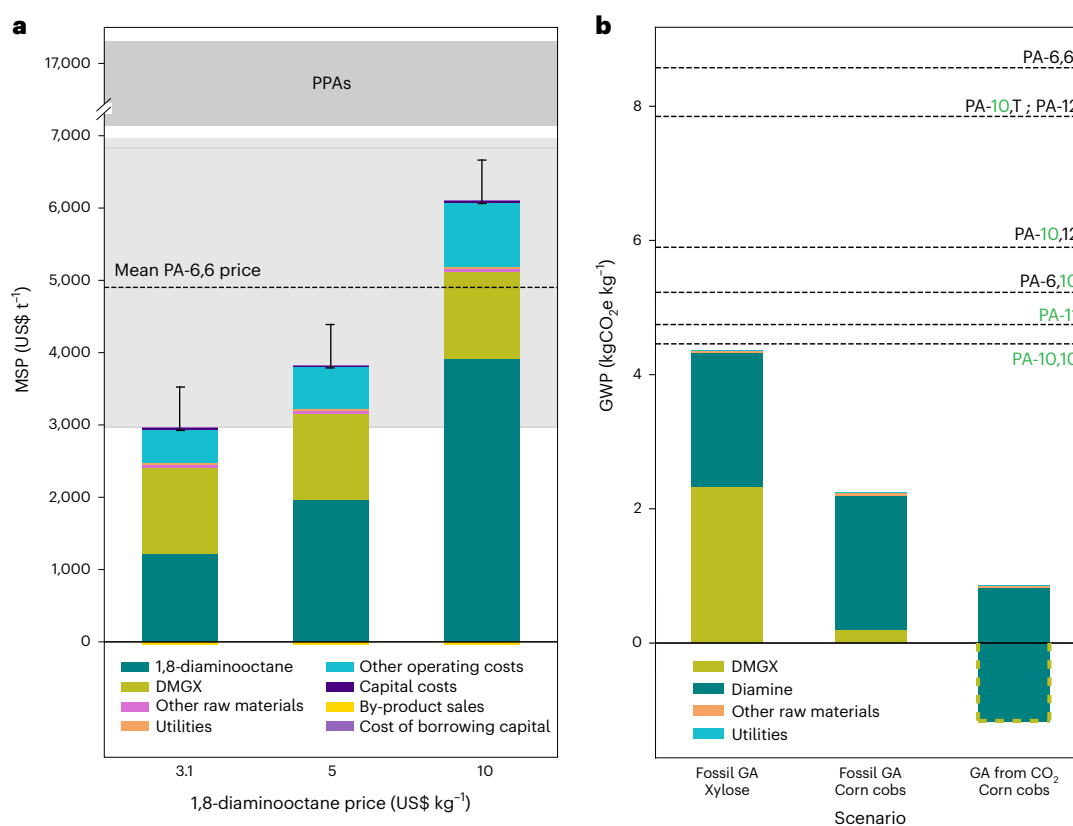


Fig. 5 | TEA and LCA of PA-8, DGX production. a, MSP of PA-8, DGX produced from DMGX (derived from commercial xylose) and 1,8-diaminooctane under various economic scenarios. The black dashed line in the left figure is the mean price for PA-6,6, and the shaded light grey area is the average price range, as reported by various sources^{14,15}. The darker shaded area corresponds to the typical price ranges for PPAs from Alibaba¹⁶. The error bars correspond to sensitivity of the MSP to the upper and lower price range for DMGX under various economic scenarios (different internal rates of return and xylose prices), as previously reported¹⁹. Cost of borrowing capital is calculated through

the weighted average cost of capital. **b**, GWP of PA-8, DGX for three different scenarios and a GWP of the diamine equivalent to that of 1,6-hexanediamine. The various scenarios consider DMGX production using fossil-based GA or CO₂-based GA and its reaction with either commercial xylose or xylan in corn cobs. The uptake of atmospheric CO₂ during the growth of corn cobs and use of CO₂-based GA makes the production of DMGX carbon negative and leads to the negative baseline. Black dashed lines are reported GWPs of other fossil or bio-based polyamides, with green text indicating the polyamides or monomers that are bio-based³⁵.

August 2022 (refs. 29,30), US\$5 kg⁻¹ and US\$10 kg⁻¹ (upper bound on Alibaba.com³¹). The price of DMGX was taken from a previous TEA that we had performed, which used the price for production from commercial xylose¹⁹. This cost would probably be reduced by using corn cobs as the feedstock. In all scenarios, the MSP of PA-8, DGX was within the market price range for nylon 66 in 2022 (light grey shaded area)^{14,15} and was far below the market price of unreinforced, high-performance PPAs (dark grey shaded area). The difference in the MSPs at the break-even point reported here and the actual market value of the polyamides corresponds to the potential for profitability.

To assess the sustainability of these materials, we performed a comparative cradle-to-gate life-cycle analysis (LCA) of PA-8, DGX along with PA-6, PA-6,6 and the bio-based PA-6,10 and PA-10,10 polyamides commercialized by Evonik under the name Vestamid Terra (see Supplementary Information 2.2 for the detailed LCA methodology)³². The GWP of PA-8, DGX was controlled mainly by the GWPs of the constituent monomers, DMGX and 1,8-diaminooctane (Fig. 5b). In this study, three main scenarios were considered for the production of DMGX. The first scenario considered DMGX production from commercial, purified xylose and fossil GA. The second considered DMGX production directly from corn cobs without co-valorization of the lignin or cellulose fractions (as previously demonstrated¹⁹) and fossil GA. Last, considering that CO₂-derived GA may soon be available commercially, we also considered this source of GA combined with the use of corn cobs as the most optimistic

scenario. Even when using fossil GA and purified xylose for production of DMGX, the GWP of PA-8, DGX was estimated to be 56% lower than that of nylon 66 and lower than other bio-based polyamides. In the likely scenario of producing DMGX from corn cobs with fossil GA, a 75% reduction in GWP from nylon 66 was expected, which is almost half of the GWP of the closest bio-based polyamide, PA-10,10. If GA is successfully produced from CO₂, the GWP of these materials could be less than 1 kgCO₂e kg⁻¹. Due to lack of available data, the GWP of 1,8-diaminooctane was assumed to be equal to that of 1,6-diaminohexane in the aforementioned scenarios. However, various scenarios were also considered to understand the sensitivity of the LCA to the sourcing of the diamine (see Supplementary Information 2.2, Supplementary Fig. 30 and Supplementary Table 4). In the worst-case scenario we considered, where the GWP of 1,8-diaminooctane is assumed to be equal to the co-invent entry for general nitrogen-containing pesticides (as 1,8-diaminooctane is used industrially as an intermediate for pesticide manufacturing), the GWP of the fossil GA/corn cob scenario increased to 4.15 kgCO₂e kg⁻¹ from 2.19 kgCO₂e kg⁻¹. If instead, 1,8-diaminooctane was sourced renewably by fermentation, we estimated the GWP of this scenario to be closer to 1.53 kgCO₂e kg⁻¹.

We also considered other environmental impact categories besides GWP³³ when analysing the overall sustainability of our material. By doing so, we observed that producing our material partially displaced the environmental burden from global warming to other

categories (Supplementary Fig. 30), as is common with bio-based solutions³³. Notably, the indicators for natural land transformation and ecotoxicity were higher for bio-based polyamides than for petro-based PA-6,6 due to farming. However, PA-8,DGX made from agricultural wastes reduced this burden compared with other bio-based polyamides that grow oil crops solely for this purpose (for example, polyamides derived from castor oil). Using agricultural residues rather than plant-based oils considerably lowers impacts on terrestrial acidification, freshwater eutrophication, marine ecotoxicity and fossil-fuel depletion.

Discussion

While using bio-based alternatives as drop-in replacements for highly deoxygenated, fossil-based plastic precursors is easier in the short term, this approach generally leads to low biomass utilization efficiency²². Considering the limited availability of renewable carbon on our planet, it is crucial to shift our focus towards redesigning the chemical industry for its efficient use rather than attempting to retrofit the petrochemical industry with renewable carbon through inefficient methods. However, developing chemicals and plastic precursors that can rival fossil-based counterparts in terms of both cost and performance while efficiently utilizing all fractions of non-edible biomass poses substantial challenges. By simultaneously retaining natural performance structures found within biomass (for example, carbohydrate cycles) in the final products, and preventing degradation during pretreatment via chemical stabilization strategies, we are able to fully valorize biomass into performance products at high efficiency (80% BUE). In addition, targeting high-value end markets with poor sustainability metrics, such as polyamides, facilitates cost competitiveness during the scaling phase. The versatility of the DMGX monomer in various material chemistries, akin to phthalate-based monomers, also leads to large addressable markets (for example, commodities) creating the opportunity to bring down costs as production scales up. Overall, achieving a substantial retention of the carbohydrate cycle within the polymer backbone (incorporation of 97% of the weight of the original xylose molecule), co-producing a stabilized lignin and a cellulose pulp and enabling CO₂ incorporation into a durable, long-lasting, recyclable material via GA offer a straightforward route towards sustainable performance plastics.

Methods

Chemicals and materials

A list of all chemicals, materials and equipment can be found in the Supplementary Information sections 1.1–1.3.

Preparation of DMGX

DMGX was produced in the same manner as previously described¹⁹. The single stereoisomer (1S-DMGX) was produced via crystallization in methanol (5 ml g⁻¹ DMGX) by heating to a boil and slowly allowing to cool to room temperature and leaving overnight. The crystals were then filtered and washed with methanol at -20 °C and dried on a Schlenk line. The batch of 1S-DMGX crystals used for the synthesis of the polyamides in the main text had a purity of 99.7% ± 0.3% by quantitative NMR in triplicate (see Supplementary Information 1.5.3 for NMR methods). The 4-stereoisomer mixture of DMGX used for the scaled syntheses was purified by recrystallization in ethanol using a new optimized procedure. The distilled 4-stereoisomer oil was dissolved in ethanol (7 ml g⁻¹ DMGX) at 50 °C in a 20 l jacketed glass reactor (10 l reaction volume) and insulated with aluminium foil. The mixture was cooled to 42 °C using a Julabo circulating thermostat at which point the crystallization was seeded with 4S-DMGX crystals with slow stirring. The crystallizer was then cooled to -10 °C at a rate of 0.07 °C min⁻¹. The crystals were filtered, washed with ethanol at -20 °C and dried on a Schlenk line. Dried DMGX crystals were recovered at 83% yield with a purity of >99.6% (by quantitative NMR).

General procedure for the preparation of 1S-poly(alkylene xylosediglyoxylamides)

Dried 1S-DMGX (2 S, 5 S isomer; see Cambridge Crystallographic Data Centre deposition number CCDC 2121378) and dry diamine were charged at 1/1.02 molar ratio in a three-neck round-bottom flask. The diamine was added in a slight excess to compensate for losses of amine due to volatilization at the beginning of the reaction. Triphenyl phosphite was then added to the reaction mixtures at 0.5 wt% with respect to DMGX. The round-bottom flask was then equipped with an overhead mechanical stirrer, a nitrogen inlet and Vigreux distillation tube outlet (see photo in Supplementary Information 1.4.2). The Vigreux column was added to help prevent losses of diamine. The receiving flask of the distillation tube was attached to an oil bubbler and a vacuum line and placed in liquid nitrogen. Before heating, the system was purged with N₂/vacuum five times. The reaction was then heated to 140 °C under a slight positive pressure of nitrogen in an oil bath at which point the DMGX and diamine rapidly reacted to form a white, salt-like solid with a rapid release of methanol. Stirring was then stopped, and the reaction temperature was then increased to 250 °C under continuous nitrogen flow. As the reaction approached 250 °C, the white salt melted into a viscous orange melt and stirring was resumed. When methanol was no longer visibly produced from the reaction, vacuum was slowly applied over 30 min to drive the polycondensation. Vacuum pressures of -0.01–0.10 mbar were used during this operation. After -2 h under vacuum, stirring started to become inefficient, and the reaction was stopped. The polymers were recovered either by pulling fibres from the melt under nitrogen flow using a glass pipette or by breaking the reaction flask (the polyamide does not stick to the glass). Exact compositions, reaction times, temperatures and yields for each of the 1S polymers are listed in Supplementary Information 1.4.2. See Supplementary Figs. 1–10 for NMR spectra and Supplementary Fig. 11 for MALDI-TOF-MS spectra of each of the polymers and the Zenodo link³⁴ to download the full characterizations.

Procedure for the large-scale preparation of 4S-poly(alkylene xylosediglyoxylamides)

For the larger-scale synthesis of the polyamides, the 4S-DMGX crystals produced via ethanol recrystallization were polymerized with diamines in the same manner as described for the single-isomer polymers except in a 1 l stainless steel, jacketed Buchi polyclave reactor with sight glass (see picture in Supplementary Information 1.4.3). The reactor was equipped with a 300 Ncm magnetically coupled overhead stirrer, a pressure gauge, a low-pressure (-1 bar) N₂ inlet, a high-pressure (5 bar) N₂ inlet, a burst disc (10 bar) and a Vigreux/distillation tube outlet connected to an oil bubbler and vacuum pump. The polymer was discharged via the bottom valve with -2 bar positive pressure of N₂ under a stream of N₂ to prevent oxidation. The reactor was then cooled to room temperature under N₂, and the remaining polymer inside the reactor was recovered by carefully freezing with liquid nitrogen and breaking with hammer and chisel. For exact compositions, conditions and yields of the polymerization, see the table in Supplementary Information 1.4.3. Yields are lower than in the glass reactors as some of the polyamide coating the 1 l reactor was not recovered.

Mechanical recycling

For the mechanical recycling study, the 4S PA-10,DGX was extruded as detailed in the 'Twin-screw extrusion' section. Twenty grams of extrudate were kept aside for characterization, and the remainder was re-dried and extruded again under the same conditions. This was repeated over a total of three cycles of extrusion. The material after each extrusion cycle was injection moulded as described in the 'Injection moulding' section for characterization by tensile testing.

Chemical recycling

The 4S PA-8, DGX was dried on a Schlenk line at 90 °C overnight before depolymerization reactions. Depolymerization reactions were conducted in heavy-walled microwave reaction vials. A stock solution was prepared consisting of 1 M H₂SO₄ in dry methanol with 20 g l⁻¹ biphenyl (99.5% purity) as internal standard for GC. A typical reaction contained 0.5 g 4S PA-8, DGX and 5 ml stock solution and an oval type stir bar. The vials were sealed with a crimp septum lid and fully immersed in an oil bath at 100 °C. Samples (50 µl) were withdrawn by gas-tight syringe through the septum after cooling and diluted in 1 ml methanol. Vials were quickly weighed between each sample to ensure no mass loss due to punctured septa. Samples were filtered (0.2 µm) and injected on the GC-FID. For determination of 1,8-diaminooctane yields, the same reactions were performed except using deuterated sulfuric acid and deuterated methanol, and quantitative NMR was performed using biphenyl as an internal standard. The alpha protons adjacent to the free amine were integrated to calculate yields once all traces of amide linkages had disappeared, ensuring that full depolymerization had occurred and we were not integrating polymer or oligomer end groups.

The chemical recycling reactions were then scaled to the 5 g polymer scale using the same conditions as those described in the preceding paragraph (5 g polymer and 50 ml of 1 M H₂SO₄ in dry methanol at 100 °C for 3 h) except in 100 ml, heavy-walled, glass reactors and without internal standard (to exclude from the separations work-up). Two reactions were performed in parallel with DMGX yields of 89.71% and 82.64% (by GC-FID with biphenyl internal standard added to GC vial), respectively. The reaction mixtures were then combined and 700 ml DCM was added and stirred when a white solid began to precipitate (Supplementary Fig. 26c). The solid was filtered, washed with DCM and dried (7.94 g; see Supplementary Fig. 28 for NMR). The filtrate was then concentrated to ~400 ml and was washed with water, followed by saturated sodium bicarbonate and brine (300 ml each; see Supplementary Fig. 26d). The DCM phase was then dried with anhydrous magnesium sulfate, filtered and dried to give the crude DMGX (6.07 g; see Supplementary Fig. 29 for NMR). The white solid containing the diamine sulfate salt was then basified in 1 M KOH (250 ml) and stirred (pH = 14). The basified solution was then extracted three times with 250 ml DCM. The DCM phase was then dried with anhydrous magnesium sulfate, filtered and evaporated to give the pure 1,8-diaminooctane (2.4 g; see Supplementary Fig. 28 for NMR). The crude DMGX was then recrystallized in ethanol (6 ml g⁻¹ DMGX, 37 ml) by heating to 60 °C, allowing to cool to room temperature with slow stirring then cooling on ice to 4 °C, followed by an ice/salt bath to -10 °C. The crystals were filtered, washed with -20 °C ethanol and dried on a Schlenk line (5.32 g; see Supplementary Fig. 29 for NMR).

HPLC analysis

A pH 2 HPLC (see Supplementary Information 1.3 for equipment details) was used for the quantification of GA, xylose and diglyoxylic acid xylose isomers using a BioRad Aminex HPX-87H column (300 mm × 7.8 mm) and Micro-Guard Cation H+ guard column. A pH 2 water mobile phase (5 ml of 1 M H₂SO₄ diluted to 1 l with MilliQ water) was used with a flow rate of 0.6 ml min⁻¹, with a 20 µl injection volume and a column temperature of 60 °C.

GC-FID analysis

Yields of DMGX were determined by GC using a biphenyl internal standard. A calibration curve of DMGX (99.7%, purity determined by quantitative NMR in triplicate) with a constant concentration of biphenyl (99.5% purity) was injected on GC three times and averaged. The molar ratio of DMGX to biphenyl was plotted against the molar ratio DMGX FID area to the biphenyl FID area. This was used to quantify the DMGX yields in the depolymerization reactions containing a known amount of biphenyl internal standard. See Supplementary Information 1.5.2 for the GC operating parameters.

NMR analysis

The ¹H-NMR, ¹³C-NMR, HSQC-NMR, COSY-NMR and HMBC-NMR spectra were acquired with 64, 1,024, 32, 32 and 16 scans, respectively, in a Bruker Avance III 400 MHz spectrometer with BBFO-plus probe. The relaxation delay (d1) was set at 2 seconds for all experiments except for quantitative NMR for which a d1 of 60 seconds was used. Samples were analysed at concentrations from 10 to 50 mg ml⁻¹. Quantitative NMR was performed in triplicate with 1,4-dinitrobenzene, or 1,2,4,5-tetrachloro-3-nitrobenzene TraceCert, as an internal standard.

MALDI-TOF-MS

A MALDI-TOF-MS of the synthesized polymers was performed on an Autoflex Speed TOF mass spectrometer (Bruker Daltonics) equipped with a Bruker smartbeam TM-II laser (355 nm wavelength) and operated in the linear positive mode. Polymers were dissolved in 1,1,1,3,3,3-hexafluoro-2-propanol (HFIP) at a concentration of 1 mg ml⁻¹. Matrix solution of trans-2-[3-(4-tert-butylphenyl)-2-methyl-2-propenylidene] malononitrile was prepared at 20 mg ml⁻¹ in tetrahydrofuran. KI and NaTFA salts were prepared at 1 mg ml⁻¹ in EtOH. Each sample was mixed with matrix and salts as a (1/10/1) volume ratio, and 1 µl was deposited on an MTP 384 ground steel BC target plate (Bruker) and allowed to dry again at room temperature. Each spectrum was collected with a minimum of 2,000 shots. For each measurement, the spectra were manually processed using flexAnalysis 3.4 Compass 1.4 (Bruker Daltonics). Calibration of linear mode was performed using the Bruker Protein Standard I.

SEC-MALS

Sample dissolution in HFIP/CF₃COOK (0.05 M) was carried out for 1 day (total sample concentration was 2–5 mg ml⁻¹). All samples were filtered through a 0.45 µm polytetrafluoroethylene syringe filter and analysed using a SEC-MALS approach. To ensure a high measurement accuracy, a full system maintenance was performed before analysis: detectors were recalibrated according to standard procedures, and normalization coefficients for the MALS detector were adjusted on the basis of the analysis of polymethylmethacrylate narrow standards. Data were processed using Astra 7 software. The dn/dc values were estimated from the refractive index signal assuming 100% mass recovery. See Supplementary Information 1.5.5 for the SEC-MALS operating parameters.

DSC

Glass transition temperatures (T_g) of dried, powdered polymer samples were measured under a nitrogen atmosphere. All glass transition temperatures were determined from the second temperature scan after any thermal history was eliminated in the first scan. Heating and cooling rates were 10 °C min⁻¹ and 5 °C min⁻¹, respectively, for all scans. No melting peaks were observed between 25 °C and 260 °C for any of the samples. Approximately 10 mg polymer sample was used for each analysis. Glass transition temperatures were determined by the absolute maximum of the first derivative of the heat flow versus sample temperature curves. See Supplementary Information 1.5.6. for the DSC temperature programme.

TGA

The polymer degradation onset temperatures (T_{onset}) and maximum degradation rate temperatures (T_{max}) of dried, powdered polymer samples (~10 mg) were measured. Samples were heated under a nitrogen atmosphere (50 ml min⁻¹) from 30 °C to 900 °C at a rate of 10 °C min⁻¹. Degradation onset temperature indicates the temperature at which a 5% mass loss was observed in the sample, and the maximum degradation rate temperature is the temperature of the maximum in the first derivative of the percentage mass loss versus temperature curves. See Supplementary Information 1.5.7 for the TGA temperature programme.

Compression moulding

Compression moulding of the 1S PA and 4S PA grades were performed on a Lauffer vacuum-assisted hot press. Specimens were produced for DMA, water absorption and tensile testing using the temperature programmes detailed in Supplementary Information 1.5.8. Before compression moulding, the polyamides were dried at 80 °C for 24 h. The polyamides were hot pressed for 10 min in a vacuum environment under 60 N cm⁻² bar of pressure at 220–250 °C, depending on the T_g of the material.

Dynamic mechanical thermal analysis

The DMA was performed using a Q850 DMA (TA Instruments) with an RH accessory, operating in tension mode. Polyamide bars (25 mm (length) × 5 mm (width) × 0.75 mm (thickness)) were conditioned at test humidity (0%, 50% and 100% RH) for at least 72 h before DMA analysis. Mechanical properties were measured from 25 °C up to 200 °C (or sample breaking point), with a free length of 10 mm, at a heating rate of 1 °C min⁻¹ at 0%, 50% and 100% RH. A preload force of 0.01 N was applied to assure sample stiffness, while an oscillating strain of 0.05% was applied at a frequency of 1 Hz during analysis. The DMA-RH chamber was kept at the desired humidity level (0%, 50% or 100%) for 30 min before measurement.

Rheological testing

Rheological experiments were performed on a DH-R2 rheometer using an environmental test chamber and a stainless steel 25 mm parallel plate geometry under a nitrogen flow (10 ml min⁻¹). The polymer samples were dried at 120 °C under vacuum for 24 h before measurement. An amplitude sweep was performed at 250 °C and 10 rad s⁻¹ to determine the linear viscoelastic region of the 4S PA-10, DGX samples. A 1% strain was selected for the frequency-sweep experiments. A frequency sweep from 0.05 rad s⁻¹ to 600 rad s⁻¹ at 250 °C was performed with collection of 10 data points per decade. The measurement gap was set to 1,000 µm, and samples were trimmed at 1,050 µm before starting tests.

Tensile strength testing

Tensile tests of 5A (ISO (International Organization for Standardization) 527-2) specimens were performed following the ISO 527 standard on a universal testing machine equipped with a 1 kN load cell. A constant head displacement rate of 1 mm min⁻¹ was applied to the specimen, and strain was recorded using mechanical extensometers. Before testing, specimens were conditioned in accordance with ISO 527 standard of 23 °C and 50% RH for 24 h. For tensile testing of dried specimen, the specimen was dried until constant mass at 80 °C for 48 h, allowed to cool to room temperature under vacuum and then immediately tested upon removal from the oven and cooled to room temperature. Mechanical properties of the 1S PA-6, DGX polymer were not measured due to defects in tensile specimen caused by bubble formation.

Injection moulding

Injection moulding of the 4S PA-10, DGX tensile specimen (ISO 527-2-1BA) was performed in a HAAKE Minjet II micro piston injection moulder. The injection moulding was conducted with a cylinder temperature of 260 °C, a mould temperature of 117 °C, an injection pressure of 1,000 bar for 7 seconds followed by a post-injection pressure of 450 bar for 5 seconds.

Water absorption

Water absorption tests were performed following method 4 of the ISO 62 standard. Specimens used for this experiment were similar to those used for DMA. After being dried for 24 h at 80 °C, they were stored in a Heraeus Vötsch HC7015 environmental chamber set at 50% RH and 23 °C. The mass of each specimen was recorded every 24 h until saturation was reached.

Twin-screw extrusion

Twin-screw extrusion of the 4S PA-10, DGX was performed in a Haake process 11 parallel twin-screw extruder using 11 mm diameter co-rotating twin screws with two mixing sections and one discharge section. The screws had eight sections, each with an L/D of 5, and a total L/D of 40. A rod die with a 2 mm diameter was used to extrude polyamide filament, which was subsequently water cooled and pelletized using a HAAKE Process 16 Varicut pelletizer. Polyamide pellets were dried at 120 °C for at least 12 h before extrusion. Extrusion was performed at 250 °C across all zones at 125 RPM with a 1.5–2.5 g min⁻¹ feed rate.

3D printing via fused-filament fabrication

The 4S PA-10, DGX filament was produced by first extruding dried virgin material with 0.1 wt% black masterbatch (OM0055 UN0055 deep black) in the process 11 extruder and pelletized as detailed in the preceding extrusion section. The pellets were then dried overnight at 120 °C and extruded into a uniform filament with 1.75 mm diameter at 250 °C using a 3Devo precision 450 filament maker. Finally, the filament was dried overnight at 90 °C and printed using a Prusa i3 MK3S 3D printer with a nozzle temperature of 275 °C and a bed temperature of 110 °C (needed to prevent warping). Double stick tape was used to ensure adhesion to the bed. The 3D model used for printing the iPhone case is available via Thingiverse at <https://www.thingiverse.com/thing:3874300> and is licensed under the Creative Commons Attribution license by the user 'semac'.

Gas barrier analysis

The oxygen permeances (or oxygen transmission rate) of the polymers were measured on samples cut from hot-pressed film using an Oxygen Permeation Analyzer–Systech Instrument Model 8001 with sensitivity equal to 0.008 cm³ m⁻² d⁻¹ bar⁻¹. The area of the samples was 5 cm², and oxygen transmission rate tests were carried out at 23 °C under 50% RH and 1 bar of oxygen pressure. Two samples were measured simultaneously using the two chambers of the instrument. The results were normalized to a film thickness of 100 µm.

The water vapour transmission rates of the polymers were measured on samples cut from hot-pressed film using an electrolytic P₂O₅ sensor (Systech 7001) with a measurement limit of 0.02 g m⁻² d⁻¹. The area of the samples was 5 cm², and the tests were carried out at 37.8 °C under 90% RH. Two samples were measured simultaneously using the two chambers of the instrument. The two chambers were purged with nitrogen until baseline stabilization, and the permeation test was initiated by exposing one side of the film to a flow of pure water vapour. The results were normalized to a film thickness of 100 µm.

TEA and LCA

Detailed methods for the TEA and LCA analyses are described in Supplementary Information 2.1 and 2.2, respectively.

Reporting summary

Further information on research design is available in the Nature Portfolio Reporting Summary linked to this article.

Data availability

All data needed to support the findings of this study are included in the main text or in the Supplementary Information. All of the data associated with the Article have been deposited³⁴ with Zenodo at <https://zenodo.org/record/8321485>. The Aspen Plus NIST ThermoData Engine was used in the development of the TEA analysis, and the Ecoinvent Database version 3 was used for sustainability metrics in the LCA analysis (with relevant metrics reported in Supplementary Table 5 and full analyses available for download on Zenodo).

References

1. Werpy, T. & Petersen, G. *Top Value Added Chemicals from Biomass: Volume I—Results of Screening for Potential Candidates from Sugars and Synthesis Gas* DOE/GO-102004-1992, 15008859 (OSTI, 2004).
2. Cao, M., Zhang, C., He, B., Huang, M. & Jiang, S. Synthesis of 2,5-furandicarboxylic acid-based heat-resistant polyamides under existing industrialization process. *Macromol. Res.* **25**, 722–729 (2017).
3. Cousin, T., Galy, J., Rousseau, A. & Dupuy, J. Synthesis and properties of polyamides from 2,5-furandicarboxylic acid. *J. Appl. Polym. Sci.* **135**, 45901 (2018).
4. Fehrenbacher, U. et al. Synthese und Charakterisierung von Polyestern und Polyamiden auf der Basis von Furan-2,5-dicarbonsäure. *Chem. Ing. Tech.* **81**, 1829–1835 (2009).
5. Kamran, M., Davidson, M. G., de Vos, S., Tsanakis, V. & Yeniad, B. Synthesis and characterisation of polyamides based on 2,5-furandicarboxylic acid as a sustainable building block for engineering plastics. *Polym. Chem.* **13**, 3433–3443 (2022).
6. Mao, L., Pan, L., Ma, B. & He, Y. Synthesis and characterization of bio-based amorphous polyamide from dimethyl furan-2,5-dicarboxylate. *J. Polym. Environ.* **30**, 1072–1079 (2022).
7. Luo, K., Wang, Y., Yu, J., Zhu, J. & Hu, Z. Semi-bio-based aromatic polyamides from 2,5-furandicarboxylic acid: toward high-performance polymers from renewable resources. *RSC Adv.* **6**, 87013–87020 (2016).
8. Yamazaki, N., Matsumoto, M. & Higashi, F. Studies on reactions of the N-phosphonium salts of pyridines. XIV. Wholly aromatic polyamides by the direct polycondensation reaction by using phosphites in the presence of metal salts. *J. Polym. Sci. Polym. Chem. Ed.* **13**, 1373–1380 (1975).
9. Mitiakoudis, A. & Gandini, A. Synthesis and characterization of furanic polyamides. *Macromolecules* **24**, 830–835 (1991).
10. Jiang, Y., Maniar, D., Woortman, A. J. J., Alberda van Ekenstein, G. O. R. & Loos, K. Enzymatic polymerization of furan-2,5-dicarboxylic acid-based furanic-aliphatic polyamides as sustainable alternatives to polyphthalamides. *Biomacromolecules* **16**, 3674–3685 (2015).
11. Jiang, Y., Maniar, D., Woortman, A. J. J. & Loos, K. Enzymatic synthesis of 2,5-furandicarboxylic acid-based semi-aromatic polyamides: enzymatic polymerization kinetics, effect of diamine chain length and thermal properties. *RSC Adv.* **6**, 67941–67953 (2016).
12. Li, H. et al. Synthesis of succinic acid-based polyamide through direct solid-state polymerization method: avoiding cyclization of succinic acid. *J. Appl. Polym. Sci.* **138**, 51017 (2021).
13. Wernet, G. et al. The ecoinvent database version 3 (part I): overview and methodology. *Int. J. Life Cycle Assess.* **21**, 1218–1230 (2016).
14. *Nylon 66, PA 66 Prices* (Smartech Global Solution Ltd., 2016).
15. *PA66 (Nylon 66) Price Trends and Forecast* (Procurement Resource, 2023).
16. *Amodel PPA Manufacturers, Suppliers and Exporters* (Alibaba.com, 2023).
17. Cywar, R. M. & Beckham, G. T. Producing performance-advantaged bioplastics. *Nat. Chem.* **14**, 967–969 (2022).
18. Questell-Santiago, Y. M., Galkin, M. V., Barta, K. & Luterbacher, J. S. Stabilization strategies in biomass depolymerization using chemical functionalization. *Nat. Rev. Chem.* **4**, 311–330 (2020).
19. Manker, L. P. et al. Sustainable polyesters via direct functionalization of lignocellulosic sugars. *Nat. Chem.* **14**, 976–984 (2022).
20. Bertella, S. et al. Extraction and surfactant properties of glyoxylic acid-functionalized lignin. *ChemSusChem* **15**, e202200270 (2022).
21. Iffland, K., Raschka, A. & Carus, M. *Definition, Calculation and Comparison of the 'Biomass Utilization Efficiency (BUE)' of Various Bio-based Chemicals, Polymers and Fuels* (Hürth, 2015); <https://renewable-carbon.eu/publications/product/nova-paper-8-on-bio-based-economy-definition-calculation-and-comparison-of-the-biomass-utilization-efficiency-bue-of-various-bio-based-chemicals-polymers-and-fuels-%e2%88%92-full-version/>
22. Manker, L. P., Jones, M. J., Bertella, S., Behaghel De Bueren, J. & Luterbacher, J. S. Current strategies for industrial plastic production from non-edible biomass. *Curr. Opin. Green Sustain. Chem.* **41**, 100780 (2023).
23. Schmid, M. et al. Properties of whey-protein-coated films and laminates as novel recyclable food packaging materials with excellent barrier properties. *Int. J. Polym. Sci.* **2012**, 562381 (2012).
24. Wypych, G. *Handbook of Polymers* (Elsevier, 2016).
25. Schall, C., Altepetter, M., Schöppner, V., Wanke, S. & Kley, M. Material-preserving extrusion of polyamide on a twin-screw extruder. *Polymers* **15**, 1033 (2023).
26. Uekert, T. et al. Technical, economic, and environmental comparison of closed-loop recycling technologies for common plastics. *ACS Sustain. Chem. Eng.* **11**, 965–978 (2023).
27. Schyns, Z. O. G., Patel, A. D. & Shaver, M. P. Understanding poly(ethylene terephthalate) degradation using gas-mediated simulated recycling. *Resour. Conserv. Recycl.* **198**, 107170 (2023).
28. *Optimizing Polymeric Materials with Rheological Analysis* (AZoNetwork, 2021).
29. *Alerts, I. Hexamethylenediamine Prices—Historical & a Forecast Data in Several Countries* (Intratec Solutions, LLC, 2019).
30. van Breugel, M. *Hexamethylenediamine Price Index* (Business Analytiq, 2020).
31. Factory Supply 1,8-Diaminooctane. *Alibaba.com* https://www.alibaba.com/product-detail/factory-supply-1-8-Diaminooctane-CAS_1600717862393.html?spm=a2700.galleryofferlist.normal_offer.d_title.6c9b7998kYbTj5 (2023).
32. Brehmer, B. *Life Cycle Assessment of Biobased Polyamides VESTAMID® Terra* (Evonik Industries AG, 2023).
33. Bachmann, M. et al. Towards circular plastics within planetary boundaries. *Nat. Sustain.* **6**, 599–610 (2023).
34. Manker, L. P. et al. Performance polyamides built on a sustainable carbohydrate core [Data set]. *Zenodo* <https://doi.org/10.5281/zenodo.8321485> (2022).
35. Brehmer, B. in *Bio-Based Plastics* (ed. Kabasci, S.) 275–293 (Wiley & Sons, 2013).

Acknowledgements

This work was supported by the Swiss National Science Foundation through grant CRSII5_180258 (J.S.L., L.P.M., M.A.H., M.J.J., K.P. and Y.K.) and the National Competence Center Catalysis (grant no. 51NF40_180544, J.S.L., L.P.M., M.A.H., M.J.J., K.P. and Y.K.), and under the Marie Skłodowska-Curie grant agreement no. 945363 (M.J.J.), by EPFL (partly through the Tech4Dev programme, J.S.L. and M.A.H.), the ISCF Smart Sustainable Plastic Packaging fund (NE/V01045X/1, M.P.S. and K.K.) and the Sustainable Materials Innovation Hub (European Regional Development Fund OC15R19, M.P.S. and K.K.). We thank M. Mokhtarimotamenishirvan for aiding in the production of the 3D-printing filament, E. Rideau and N. Diercks for assistance with the 3D printing, Z. Schyns for assistance with twin-screw extrusion and A. Schreier for assistance with gas barrier measurements. ChatGPT was used to aid with text editing but only by modifying original text written by the authors after which the text was systematically re-edited.

Author contributions

L.P.M. and J.S.L. conceived of the project and designed the research. L.P.M. performed most of the experiments and drafting of the paper. M.A.H., supervised by J.S.L. and R.M., and C.B., supervised by V.M. and

H.F., performed most of the material characterization. M.J.J. performed the techno-economic and life-cycle analyses and was supervised by F.M. and J.S.L. Y.K. assisted in the chemical recycling experiments. K.K. performed all dynamic mechanical analyses and rheological characterizations, supervised by M.P.S. K.P. assisted in the synthesis of some of the polymers. All authors contributed to editing the paper.

Funding

Open access funding provided by EPFL Lausanne.

Competing interests

The authors declare the following competing financial interests. L.P.M. and J.S.L. are inventors on a European patent application (EP19203000.5) on methods for producing the renewable monomer and polymer described here. J.S.L. is a co-founder, and M.A.H. a shareholder, of Bloom Biorenewables Ltd., which is exploring commercial opportunities for aldehyde-stabilized lignin and aldehyde-protected xyloses. The other authors declare no competing interests.

Additional information

Supplementary information The online version contains supplementary material available at <https://doi.org/10.1038/s41893-024-01298-7>.

Correspondence and requests for materials should be addressed to Jeremy S. Luterbacher.

Peer review information *Nature Sustainability* thanks Brett Helms, Youhua Tao and the other, anonymous, reviewer(s) for their contribution to the peer review of this work.

Reprints and permissions information is available at www.nature.com/reprints.

Publisher's note Springer Nature remains neutral with regard to jurisdictional claims in published maps and institutional affiliations.

Open Access This article is licensed under a Creative Commons Attribution 4.0 International License, which permits use, sharing, adaptation, distribution and reproduction in any medium or format, as long as you give appropriate credit to the original author(s) and the source, provide a link to the Creative Commons licence, and indicate if changes were made. The images or other third party material in this article are included in the article's Creative Commons licence, unless indicated otherwise in a credit line to the material. If material is not included in the article's Creative Commons licence and your intended use is not permitted by statutory regulation or exceeds the permitted use, you will need to obtain permission directly from the copyright holder. To view a copy of this licence, visit <http://creativecommons.org/licenses/by/4.0/>.

© The Author(s) 2024

Reporting Summary

Nature Portfolio wishes to improve the reproducibility of the work that we publish. This form provides structure for consistency and transparency in reporting. For further information on Nature Portfolio policies, see our [Editorial Policies](#) and the [Editorial Policy Checklist](#).

Statistics

For all statistical analyses, confirm that the following items are present in the figure legend, table legend, main text, or Methods section.

- | n/a | Confirmed |
|-------------------------------------|--|
| <input type="checkbox"/> | <input checked="" type="checkbox"/> The exact sample size (n) for each experimental group/condition, given as a discrete number and unit of measurement |
| <input type="checkbox"/> | <input checked="" type="checkbox"/> A statement on whether measurements were taken from distinct samples or whether the same sample was measured repeatedly |
| <input type="checkbox"/> | <input checked="" type="checkbox"/> The statistical test(s) used AND whether they are one- or two-sided
<i>Only common tests should be described solely by name; describe more complex techniques in the Methods section.</i> |
| <input checked="" type="checkbox"/> | <input type="checkbox"/> A description of all covariates tested |
| <input checked="" type="checkbox"/> | <input type="checkbox"/> A description of any assumptions or corrections, such as tests of normality and adjustment for multiple comparisons |
| <input type="checkbox"/> | <input checked="" type="checkbox"/> A full description of the statistical parameters including central tendency (e.g. means) or other basic estimates (e.g. regression coefficient) AND variation (e.g. standard deviation) or associated estimates of uncertainty (e.g. confidence intervals) |
| <input checked="" type="checkbox"/> | <input type="checkbox"/> For null hypothesis testing, the test statistic (e.g. F , t , r) with confidence intervals, effect sizes, degrees of freedom and P value noted
<i>Give P values as exact values whenever suitable.</i> |
| <input checked="" type="checkbox"/> | <input type="checkbox"/> For Bayesian analysis, information on the choice of priors and Markov chain Monte Carlo settings |
| <input checked="" type="checkbox"/> | <input type="checkbox"/> For hierarchical and complex designs, identification of the appropriate level for tests and full reporting of outcomes |
| <input checked="" type="checkbox"/> | <input type="checkbox"/> Estimates of effect sizes (e.g. Cohen's d , Pearson's r), indicating how they were calculated |

Our web collection on [statistics for biologists](#) contains articles on many of the points above.

Software and code

Policy information about [availability of computer code](#)

Data collection	Topspin (version 3.6.4) was used for NMR acquisition, Agilent GC OpenLab ChemStation (LTS 01.11) was used to collect GC-FID data, Agilent HPLC OpenLab ChemStation (LTS 01.11) was used to collect HPLC data, STARe Excellence Thermal Analysis Software (version 12.1) was used for DSC and TGA data collection, and TRIOS (version 5.2) was used for collection of rheology and DMA data.
Data analysis	Microsoft Excel (Version 1808) and OriginPro (2020b) were used for data analysis and plotting. MestReNova (14.3.3-3362) was used for NMR spectrum analysis, Astra 7 was used for GPC chromatogram analysis, Agilent GC OpenLab ChemStation (LTS 01.11) was used for GC-FID chromatogram analysis, and Agilent HPLC OpenLab ChemStation (LTS 01.11) was used for HPLC chromatograms analysis.

For manuscripts utilizing custom algorithms or software that are central to the research but not yet described in published literature, software must be made available to editors and reviewers. We strongly encourage code deposition in a community repository (e.g. GitHub). See the Nature Portfolio [guidelines for submitting code & software](#) for further information.

Data

Policy information about [availability of data](#)

All manuscripts must include a [data availability statement](#). This statement should provide the following information, where applicable:

- Accession codes, unique identifiers, or web links for publicly available datasets
- A description of any restrictions on data availability
- For clinical datasets or third party data, please ensure that the statement adheres to our [policy](#)

All data needed to support the findings of this study are included in the main text or in the supplementary information. All of the data associated with the Article have been deposited with Zenodo at <https://zenodo.org/record/8321485>. The zenodo dataset will be published upon publication of the article. The Aspen Plus NIST ThermoData Engine was used in the development of the TEA analysis and the Ecoinvent Database version 3 was used for sustainability metrics in the LCA analysis.

Human research participants

Policy information about [studies involving human research participants and Sex and Gender in Research](#).

Reporting on sex and gender	Not applicable
Population characteristics	Not applicable
Recruitment	Not applicable
Ethics oversight	Not applicable

Note that full information on the approval of the study protocol must also be provided in the manuscript.

Field-specific reporting

Please select the one below that is the best fit for your research. If you are not sure, read the appropriate sections before making your selection.

Life sciences Behavioural & social sciences Ecological, evolutionary & environmental sciences

For a reference copy of the document with all sections, see [nature.com/documents/nr-reporting-summary-flat.pdf](https://www.nature.com/documents/nr-reporting-summary-flat.pdf)

Ecological, evolutionary & environmental sciences study design

All studies must disclose on these points even when the disclosure is negative.

Study description	We synthesized a class of polyamides and performed characterization of their chemical identity as well as their material properties. We also performed end-of-life studies as well as TEA/LCA analyses.
Research sample	The samples involved running GPC, MALDI, NMR, DSC, TGA, DMA, tensile testing, gas barrier analysis, and rheological analysis on the polymeric materials. For quantification of small molecules, GC and quantitative NMR were used.
Sampling strategy	For the GPC, MALDI, NMR, DSC, TGA, Rheology and DMA analyses, single samples were measured, as is standard in the polymer community. Tensile testing was performed on 3-5 samples as variation in properties can occur due to defects in samples during processing of tensile specimen. Gas barrier analysis was performed on two samples simultaneously as is instructed by the instrument manual. GC-FID and quantitative NMR analyses were performed by repeated sampling of single chemical recycling mixtures containing an internal standard. The use of an internal standard as well as repeated sampling enables accurate quantification without the need for replicates. Deviations from a trend would indicate sampling issues and the use of an internal standard accounts for variations in GC injection volumes and sample dilutions.
Data collection	Raw data was collected from each of the instruments after measurement. Data was collected by LPM, MAH, CB, KK, KP and YK.
Timing and spatial scale	Each of these characterizations were performed on a single day.
Data exclusions	The only data exclusions were for the elongation at break values for tensile specimen where clear premature failure occurred due to physical contact with the contact extensometer knife blades (see SI Figure S33 for photo). Tensile moduli and ultimate tensile strengths were still reported for these specimen, as this phenomena only impacts elongation at break. The data exclusions are clearly indicated in red in the raw data sets uploaded to Zenodo (https://zenodo.org/record/8321485) with justification for their exclusion.
Reproducibility	As explained in the Sampling Strategy section: For the GPC, MALDI, NMR, DSC, TGA, Rheology and DMA analyses, single samples were measured, as is standard in the polymer community. Tensile testing was performed on 3-5 samples as variation in properties can occur due to defects in samples during processing of tensile specimen. Gas barrier analysis was performed on two samples simultaneously as is instructed by the instrument manual. GC-FID and quantitative NMR analyses were performed by repeated

sampling of single chemical recycling mixtures containing an internal standard. The use of an internal standard as well as repeated sampling enables accurate quantification without the need for replicates. Deviations from a trend would indicate sampling issues and the use of an internal standard accounts for variations in GC injection volumes and sample dilutions.

Randomization

Not applicable

Blinding

Not applicable

Did the study involve field work? Yes No

Reporting for specific materials, systems and methods

We require information from authors about some types of materials, experimental systems and methods used in many studies. Here, indicate whether each material, system or method listed is relevant to your study. If you are not sure if a list item applies to your research, read the appropriate section before selecting a response.

Materials & experimental systems

- | n/a | Involvement in the study |
|-------------------------------------|--|
| <input checked="" type="checkbox"/> | <input type="checkbox"/> Antibodies |
| <input checked="" type="checkbox"/> | <input type="checkbox"/> Eukaryotic cell lines |
| <input checked="" type="checkbox"/> | <input type="checkbox"/> Palaeontology and archaeology |
| <input checked="" type="checkbox"/> | <input type="checkbox"/> Animals and other organisms |
| <input checked="" type="checkbox"/> | <input type="checkbox"/> Clinical data |
| <input checked="" type="checkbox"/> | <input type="checkbox"/> Dual use research of concern |

Methods

- | n/a | Involvement in the study |
|-------------------------------------|---|
| <input checked="" type="checkbox"/> | <input type="checkbox"/> ChIP-seq |
| <input checked="" type="checkbox"/> | <input type="checkbox"/> Flow cytometry |
| <input checked="" type="checkbox"/> | <input type="checkbox"/> MRI-based neuroimaging |